

The Ionization Structure of Planetary Nebulae
X. NGC 2392

P. 40

TIMOTHY BARKER^{1,2}

Department of Physics and Astronomy
Wheaton College

Received 1989 October 3;

¹Visiting Astronomer, Kitt Peak National Observatory, National Optical Astronomy Observatories, operated by the Association of Universities for Research in Astronomy, Inc., under contract with the National Science Foundation.

²Guest observer with the International Ultraviolet Explorer Satellite, NASA grant NSG 5376.

(NASA-CR-186960) THE IONIZATION STRUCTURE
OF PLANETARY NEBULAE 10: NGC 2392 Semiannual
Report (Wheaton Coll.) 40 p CSCL 038

N90-29274

Unclass

G3/90 0303428

ABSTRACT

Spectrophotometric observations of emission-line intensities over the spectral range 1400-7200 Å have been made in six positions in the planetary nebula NGC 2392. The O^{++} electron temperature averages 14,500 K, which is 4100 K higher than the average N^+ electron temperature; this is an unusually large difference. The Balmer continuum electron temperature averages 1500 K higher than the O^{++} electron temperature, but this difference is only slightly greater than the measurement errors. As found for most of the other planetaries in this series, the $\lambda 4267$ C II line intensity implies a C^{++} abundance that is several times higher than that determined from the $\lambda 1906, 1909$ C III] lines. The discrepancy disappears if one adopts the N^+ electron temperature, rather than the O^{++} electron temperature for the C^{++} region, but both theoretical and observational evidence support the use of the O^{++} temperature. As for the other papers in this series, it is argued that the $\lambda 4267$ C II line intensity is not being interpreted correctly, perhaps because it is blended with a line from an unknown high-excitation ion. Standard equations used to correct for the existence of elements in other than the optically observable ionization stages give consistent results for the different positions that are in excellent agreement with abundances calculated using ultraviolet lines, and there is no evidence for any abundance gradient in the nebula. The logarithmic

abundances (relative to H = 12.00) are He = 10.99, O = 8.53, N = 8.04, Ne = 7.88, C = 7.62, Ar = 6.15, and S = 6.63. These abundances agree well with determinations by Aller and Keyes, except that the C abundance is a factor of 5 lower than theirs. The abundances are very similar to those found for NGC 1535 and NGC 6826 (the previous papers in this series). As for NGC 1535 and NGC 6826, the rather low abundances of He, N, and C suggest that there was little if any mixing of CNO-processed material into the nebular shell in the progenitor to NGC 2392. The O, Ne, and Ar abundances also appear to be somewhat low, suggesting that the progenitor to NGC 2392 may have formed out of somewhat metal-poor material.

Subject headings: nebulae: abundances - nebulae: individual
(NGC 2392) - nebulae: planetary - ultraviolet: spectra

I. INTRODUCTION

The previous papers in this series analyzed optical and ultraviolet observations of different positions in the planetary nebulae NGC 6720 (Barker 1980, 1982, 1987, hereafter Papers I, II, and VII, respectively), NGC 7009 (Barker 1983, hereafter Paper III), NGC 6853 (Barker 1984, hereafter Paper IV), NGC 3242 (Barker 1985, hereafter Paper V), NGC 7662 (Barker 1986, hereafter Paper VI), NGC 6826 (Barker 1988, hereafter Paper VIII), and NGC 1535 (Barker 1989, hereafter Paper IX). The purpose of these studies is to measure optical and UV emission-line intensities in the same nebular positions using similar entrance apertures. Since the ionization frequently changes drastically with position in an extended nebula, this procedure is almost essential in order to make a meaningful comparison between UV and optical measurements. The ultimate goals include the following: (1) to observe elements in more stages of ionization than is possible from optical spectra alone; this provides a check on optical ionization correction procedures, which are still needed for nebulae which are too faint to observe with the *International Ultraviolet Explorer (IUE)* satellite; (2) to get particularly accurate total abundances by averaging measurements made in different parts of the nebula, so that small differences between nebulae will become apparent; such differences can be

sensitive tests of theoretical predictions regarding CNO processing and mixing in the progenitors of planetaries; and (3) to further investigate the discrepancies found in Papers II, III, IV, V, VI, VIII, and IX between optical and UV measurements of the abundance of C^{++} ; these discrepancies need to be understood before we can have confidence in optical measurements of that important element.

I chose NGC 2392 (the "Eskimo Nebula") as the next planetary in this series because it has a fairly high surface brightness and so can be observed with reasonable exposure times using the smaller of the two *IUE* entrance apertures. In addition, it has measurable He II UV and optical emission in all positions, facilitating the difficult task of combining the UV and optical observations. Finally, there have been no recent detailed studies of the abundances in this object.

II. OBSERVATIONS

a) *Optical Observations*

The optical observations were made at Kitt Peak National Observatory in 1983 December, 1984 March, and 1987 January, using the 2.1 m telescope and the intensified image dissector scanner

(IIDS). Spectra were obtained in six different positions through a 3".4 diameter aperture (10".3 for position 6) using two grating settings covering the ranges 3400-5100 Å and 4600-7200 Å with resolutions of about 10 Å (FWHM). Both spectral regions were observed on two nights for the inner five positions and one night for position 6; offsets with respect to the central star are listed in Table 1. In Figures 1-4, the aperture positions and sizes are superimposed on contour maps provided by B. Balick. These maps are all at the same scale and were derived from 2.1m CCD images of the nebula taken in the light of H α , [O III], [N II], and He II as described by Balick (1987).

b) *Correction for Interstellar Reddening*

The amount of interstellar reddening for each position was measured by comparing the observed and theoretical intensities of the H recombination lines (the "Balmer decrement"). The resulting values of the reddening parameter, c , for each position are listed in the second row of Table 1. There is somewhat more scatter in the values of c than would be expected from measurement errors alone. Zipoy (1976) and Balick (1990) also found evidence that there is variable reddening across the nebula, and I have found some evidence for variable reddening in several planetaries (see Papers V,

VI, VII, VIII, and IX). The range in c is rather small, however (especially excluding position 1, where contamination by light from the central star may be a factor), and I decided in the end to adopt a mean value of $c = 0.13 \pm 0.04$. This value is consistent with the estimates of 0.22 by Zipoy (1976) and 0.15 by Aller and Keyes (1981), and with the value of 0.08 estimated for the direction to NGC 2392 from the H I/galaxy count study by Burstein and Heiles (1982). A value of $c = 0.13$ also leads to good agreement between the predicted and observed UV He II $\lambda 1640$ intensities (see the last two rows of Table 1 and the discussion in the next section).

The intensities listed in Table 2 have been calculated by multiplying the observed intensities by $10^{cf(\lambda)}$; the values of the interstellar reddening function $f(\lambda)$ are also listed in Table 2. Note that, as discussed above, the adopted reddening parameters lead to Balmer decrements for the six positions that are consistent with the theoretical (Brocklehurst 1971) intensities of $H\alpha$, $H\beta$, $H\gamma$, $H\delta$, $H9$, and $H10$ of 281, 100, 47, 26, 7.4, and 5.4, respectively. Two other corrections have been applied in Table 2: the intensities of $H\beta$ have been corrected for blending with He II emission, and the intensities of the $\lambda 3727$ [O II] lines have been corrected for blending with other lines as described in Paper III. Because of the brightness of the [O II] lines in NGC 2392, the blending correction was quite small,

resulting in the observed intensities being multiplied by factors of only .94, .93, .91, .95, .97, and .93, respectively.

c) Ultraviolet Observations

The ultraviolet observations were made using the small ($\approx 3''.2$ diameter) entrance aperture of the *IUE* satellite in 1986 February. Table 1 lists the *IUE* exposure numbers and times. The *IUE* offsets were made under the assumption that the center of light position measured by the *IUE* fine error sensor coincides with the central star. Since NGC 2392 is a highly symmetric object, this assumption is reasonable, but as a check, exposures were taken with both the small and large apertures centered on the assumed position of the central star. After allowing for the lower throughput of the small aperture, the observed continuum was about the same for both apertures, and it therefore seems probable that the *IUE* exposures were made within 1" to 2" of the positions given in Table 1. Position 6 was observed with the large *IUE* entrance aperture, which serendipitously fell on the outer shell of the nebula (the "parka" of the "Eskimo") when position 5 was observed with the small aperture. Only the central part of the aperture was used when the spectrum from this position was analyzed; the resulting effective entrance aperture was approximately a $10''$ square, similar to the $10.''3$

circular aperture used for the optical observations of position 6. The data were reduced in 1986 February and 1987 February at the IUE Regional Data Analysis Facility at Goddard Space Flight Center using the 1980 May calibration for the SWP camera and the December 1983 calibration (given in *IUE* Newsletter 23) for the LWP camera.

As in the previous papers in this series, putting the UV and optical observations on the same intensity scale is a difficult task because no emission lines can be observed in common. One method is to directly compare absolute flux measurements, after correcting for the difference in the areas of the entrance apertures. A check on this method is provided by the intensities of the He II lines; for the physical conditions in NGC 2392, $I(\lambda 1640)$ should equal $6.9 I(\lambda 4686)$ (Seaton 1978). The predicted and observed *fluxes* (uncorrected for interstellar extinction) are compared in the last two rows of Table 1. Considering the uncertainties inherent in comparing absolute fluxes, the agreement between these fluxes is excellent. As for all the other nebulae in this series with measurable He II emission, however, I decided that the most reliable method for combining the UV and optical observations is to require that $I(\lambda 1640) = 6.9 I(\lambda 4686)$. This method has the advantage of being unaffected by uncertainties in the photometric areas in the apertures, as well as possibly non-photometric conditions when the optical measurements were made, and it is nearly unaffected by errors in the correction for interstellar

reddening. It is important to emphasize, however, that directly combining the UV and optical observations would have given essentially the same results.

d) *Observational Errors*

The UV intensities are judged to be accurate to within a factor of 2 for the weakest lines and those marked with colons, to $\approx 40\%$ for those of intermediate intensity (between 20% and 80% of $H\beta$ and to $\approx 20\%$ for the strongest lines. While these errors may seem high, errors in electron temperatures generally have a greater effect than errors in line intensities on the accuracy of the abundances determined from collisionally excited UV lines.

Based on experience with the equipment and a comparison with between the IIDS measurements made on different nights, the intensities of the strongest optical lines are judged to be accurate to $\approx 10\%$, those weaker than half of $H\beta$ to be accurate to $\approx 20\%$, and even the faintest lines to be accurate to $\approx 30\%$.

III. TEMPERATURES, DENSITIES, AND IONIC ABUNDANCES

Calculations of the electron density (N_e), electron temperature (T_e) and ionic abundances in the different positions were made using the same methods and atomic constants as in Paper III. The results for N_e and T_e are summarized in Table 3. The Cl^{++} determination of N_e is much less reliable than the S^+ determination because the [Cl III] lines are quite faint, and the electron density in NGC 2392 is near the low density limit for this indicator; even so, the two indicators agree well. Similarly, the Ne^{3+} determination of T_e is much less reliable than the N^+ and O^{++} values because of the faintness of the [Ne IV] lines and the uncertainties in the calibration and reddening over this wavelength range. Considering these uncertainties, the Ne^{3+} determination may be said to be consistent with the other indicators. Both the N^+ and O^{++} measurements of T_e should be quite accurate in NGC 2392. The fact that the [O III] T_e averages 4100 K higher than the [N II] T_e is therefore almost certainly a result of T_e actually being higher in the regions of higher ionization. This difference is consistent with the measurements by Torres-Peimbert and Peimbert (1977), who found that the [O III] T_e averages 1.25 times higher than the [N II] T_e in planetaries (like NGC 2392) which have strong He II emission. The difference is also consistent with that measured by Aller and Keyes (1980), who

estimated an [O III] T_e of 13,100 K and an [N II] T_e of 10,000 K from integrated spectra of NGC 2392. This difference may be due to the extreme filamentary structure of NGC 2392 when studied in the light of [N II]; see Figure 3 and also the [N II] image published by Balick (1987). Apparently, much of the N^+ in NGC 2392 exists in radial "dagger-like" regions that have lower temperatures than the surrounding, more highly-ionized gas and which are also distinct kinematically (see Balick, Preston, and Icke, 1987). The Balmer continuum T_e was measured as explained in Paper V and is subject to greater uncertainties than the N^+ and O^{++} electron temperatures because of its extreme sensitivity to errors in c , uncertainties in estimating the continuum, and uncertainties in the instrumental calibration at the Balmer limit. As in Papers V, VI, VIII, and IX, however, there is no evidence that the T_e 's measured this way are systematically lower than the O^{++} T_e 's, as has been claimed for some nebulae; in fact the average value of T_e found from the Balmer continuum, 16,000 K, is 1500 K higher than that found from the [O III] lines. A similar difference was observed in other planetaries in this series; in NGC 7662, for example (Paper VI), the difference was 1200 K, which was in good agreement with the theoretical model prediction of 1460 K (Harrington, Seaton, Adams, and Lutz, 1982). Considering the uncertainties inherent in measuring the Balmer continuum T_e , I believe that the agreement with the [O III] T_e is satisfactory in NGC 2392.

The adopted values of N_e and T_e are listed in the last three rows of Table 3. The values of N_e were taken from the S^+ indicator and are consistent with the value of $N_e \approx 3000 \text{ cm}^{-3}$ measured by Aller and Keyes from integrated spectra. The calculated ionic abundances are very insensitive to errors in N_e for values of N_e this low. As in NGC 6720, a two-temperature model was adopted for NGC 2392, with the $N^+ T_e$ used for singly-ionized species and the $O^{++} T_e$ used for all others. Since the two indicators give such discordant values of T_e , this assumption has a large effect on calculated abundances, particularly for C. The validity of this method will be discussed more fully in the section on the C abundance (§ IVe).

The ionic abundances calculated using the values of N_e and T_e given at the bottom of Table 3 are listed in Table 4.

IV. TOTAL ABUNDANCES

Total abundances may be found by simply adding together all the ionic abundances or by using only optically measured ionic abundances and correcting for the presence of elements in optically unobservable stages of ionization. The former procedure would appear to be the more reliable, but unfortunately relatively small

errors in T_e will cause large errors in abundances measured from UV lines. At the very least, however, this method serves as a valuable check on the second procedure, which is commonly used when no UV data are available for a nebula. Both methods were used wherever possible, and the results are summarized in Table 4. The abundances labeled "optical" have been calculated by multiplying the optically measured ionic abundances by the listed values of i_{cf} , the ionization correction factor (the equations used to calculate i_{cf} values are given in Paper III). The abundances labeled "UV + optical" are simple sums of all the ionic abundances.

The errors assigned to the abundances in Table 4 are based on the errors estimated for the electron temperatures, densities, and ionic abundances. In most cases, the errors in T_e dominate the other sources.

The average abundances and errors based on measurements in the six positions are given in the first row of Table 5. The optical measurements were used for all elements except C (see below). For comparison, the results of a study of NGC 2392 by Aller and Keyes (1981; hereafter AK) that combines optical and UV data together with model calculations are listed in the second row. Considering the differences in observing techniques and methods of analysis, the agreement between the two studies is good, although AK found a

significantly higher C abundance. A detailed discussion is given below.

a) *Helium*

The three different He I lines agree very well, and the average He^+/H^+ abundance given in Table 4 for each position is an unweighted sum of the three measurements. The total He abundance is the sum of the He^+ and He^{++} abundances. Since He II emission is present in all positions, little if any He is expected to be in the form of He^0 . The constancy of the total measured He abundance throughout the nebula supports this conclusion. The He abundance given in Table 5 is a straight average of the six positions and is in good agreement with measurement by AC.

b) *Oxygen*

For all six positions, there is excellent agreement between the O^{++} abundances determined using the $\lambda 1661, 1666$ [O III] UV lines and those using the $\lambda 5007$ [O III] line. This fact is an indication that the UV and optical measurements have been combined correctly and that the values of T_e adopted for the O^{++} region are correct. The total

calculated O abundances for the different positions are extremely consistent. Since the i_{cf} 's vary by only about 50% across these positions, however, this agreement gives little support for the applicability of the ionization correction procedure for O. It does indicate, however, that there is little or no O abundance gradient in the nebula, even between the inner and outer envelope. The average O abundance for NGC 2392 listed in Table 5 is in excellent agreement with the determination by AK.

c) *Nitrogen*

The calculated N abundance based on the observed N^+ abundance and the optical ionization correction factors is reasonably consistent across the nebula. The resulting average N abundance given in Table 5, $(1.1 \pm 0.1) \times 10^{-4}$, is in excellent agreement with the average N abundance calculated by adding the ionic abundances, $(1.1 \pm 0.2) \times 10^{-4}$. This agreement provides further evidence that N abundances can be measured optically, even when a small fraction of the N (as little as 4% in NGC 2392) is in the optically observable form of N^+ .

d) *Neon*

The total optically measured Ne abundance is approximately constant and apparently not overestimated in the lower ionization positions (as in Papers I, IV, and VI); in NGC 2392, as in NGC 1535, NGC 3242, NGC 6826, NGC 7009, and NGC 7662, the ionization is high enough that there is little O^+ and so the different efficiencies of the O and Ne charge transfer reactions are not important (see Paper I and references therein). Adding together the ionic abundances gives an average Ne abundance of $(0.55 \pm 0.05) \times 10^{-4}$. It is reasonable that this value is slightly less than the optically determined value of $(0.76 \pm 0.05) \times 10^{-4}$, since a small fraction of the Ne is expected to be in the unobservable form of Ne^+ . In summary, the optical result is again consistent with the UV+optical measurement, although the former is to be preferred because it allows for Ne in the Ne^+ form and is less sensitive to errors in T_e . Note that the resulting average Ne abundance listed in Table 5 is fairly close to the measurement by AK.

e) *Carbon*

As in NGC 1535, NGC 3242, NGC 6720, NGC 6826, NGC 6853, NGC 7009, and NGC 7662, the C^{++} abundance inferred from the $\lambda 4267$ line

is larger than that found using the UV $\lambda 1906, 1909$ lines. The ratio of the two measurements is 9.8, 8.8, <3.2 , 7.1, 24.3, and <3.3 for positions 1-6, respectively. (It is likely that much of the scatter in this ratio is due to errors in measuring the faint $\lambda 4267$ line.) The discrepancy between the two measurements differs from that found in the other planetaries in two important respects, however.

First, the difference between the N^+ and O^{++} T_e 's in NGC 2392 is much larger than in any of the other planetaries and raises the issue of which T_e is more appropriate to C^{++} . The discrepancy between the C^{3+} abundance inferred from the $\lambda 4267$ line and that found using the UV $\lambda 1906, 1909$ lines would, in fact, essentially disappear if one adopted the N^+ T_e for the C^{++} region, rather than the O^{++} T_e . (Since the N^+ T_e 's average 4100 K lower than the O^{++} T_e 's, C^{++} abundances calculated from the highly T_e sensitive $\lambda 1906, 1909$ C III] lines would be increased by nearly a factor of 10 if the N^+ T_e 's were adopted.) The final average C abundance would then be roughly 2×10^{-4} , consistent with the measurement by AK (see Table 5). Two lines of evidence suggest, however, that it is the O^{++} T_e , rather than the N^+ T_e , that is appropriate to the C^{++} region. First, theoretical considerations (for example, the model calculations for NGC 7662 by Harrington, Seaton, Adams, and Lutz, 1982) show that, as expected from a comparison of ionization potentials, the O^{++} and C^{++} regions are coincident and closer to the central star than the N^+ region. (It

would be extremely useful, however, to have C III] images to compare with Figure 2 to see if the O^{++} and C^{++} regions really do coincide in NGC 2392, which has filamentary structure not allowed for by models.) In addition, for NGC 2392, Aller and Keyes (1980) estimated a T_e for the C^{++} region that is very close to that for the O^{++} region. Second, the comparison by Kaler (1986) of electron temperatures in thirty planetary nebulae indicated that the C^{++} T_e 's correlate much better with the O^{++} T_e 's than with the N^+ T_e 's. I believe that the weight of the evidence suggests that the O^{++} T_e 's are appropriate for the C^{++} region. I believe that NGC 2392 provides further evidence that the excitation mechanism for the $\lambda 4267$ line is not well understood. (For a more extensive discussion of this issue, see Paper VII and references therein, as well as the recent review by Clegg, 1988.) The total C abundance for each position was therefore found by summing the ionic abundances measured from the UV lines alone, assuming that the O^{++} T_e was appropriate. The resulting C abundances for the six positions are quite consistent, but, as mentioned above, the average C abundance for the whole nebula is substantially (a factor of 5) less than that measured by AK. This difference is apparently due primarily to their measuring a somewhat lower T_e for the C^{++} region (13,100 K as opposed to the average value of 14,500 K found here) and their measured intensity of the UV $\lambda 1906$, 1909 lines being somewhat greater.

A second way in which the C^{++} discrepancy in NGC 2392 differs from that in the other planetaries in this series is that, although the magnitude of the discrepancy is similar to that in the others, it is not related to projected distance from the central star. (In the other objects, the discrepancy generally decreases approximately monotonically with increasing projected distance from the central star.) NGC 2392 is unique, however, in that it has strong $\lambda 4686$ He II emission in all positions; in the other planetaries, the ionization in the outer regions was substantially lower than in the inner regions. The explanation for the lack of positional dependence of the discrepancy in NGC 2392 could therefore possibly be that, as suggested previously, the $\lambda 4267$ line is a blend of both the C II line and another line from an unknown ion whose abundance correlates with He^{++} .

f) Argon

Since most of the oxygen in NGC 2392 is in a higher ionization stage than O^+ (ionization potential: 35 ev), almost all Ar should be in a higher ionization stage than Ar^+ (ionization potential: 28 ev) and hence in the optically observable stages Ar^{++} , Ar^{3+} , and Ar^{4+} . In other words, the ionization correction factors should be only slightly greater than 1.00, which is, in fact the case. The total Ar abundances for the different positions agree within a factor of two or so, and the average Ar abundance listed in Table 5 is almost identical to that

found by AK. The equation $\text{Ar}/\text{H} = 1.5 \text{ Ar}^{++}$ (see Paper I), which is a useful factor-of-two approximation for faint planetaries where only the $\lambda 7135$ [Ar III] line is observable, gives an average Ar/H ratio of $(0.83 \pm 0.3) \times 10^{-6}$, which is a little less than a factor of two below the measured value of $(1.4 \pm 0.2) \times 10^{-6}$ (see Table 5).

g) *Sulfur*

The i_{cf} 's for S are rather small, and so the calculated S abundances should be fairly accurate. The agreement between the different positions is reasonable, but much of the scatter may be due to the sensitivity of the $\lambda 6312$ [S III] line to errors in T_e and to errors associated with deblending it from the nearby $\lambda 6300$ [O I] line. The average S abundance listed in Table 5 is consistent with the measurement by AK.

h) *Comparison of Abundances in Different Objects*

In general, the abundances in the objects in Table 5 are similar, but there are some interesting differences. The abundances of He, O, Ne, Ar, and S in NGC 2392 are quite similar to those in NGC 1535, NGC 3242, NGC 6826, and NGC 7662. The helium abundances in

these five planetaries, which are lower than in any of the other objects listed, imply that there has been little (perhaps no) enhancement of He-rich material in NGC 2392. The abundances of C and, to some extent, N, in NGC 2392, like those in NGC 1535 and NGC 6826, are lower than in the other planetaries and are in agreement with the values in the Sun and H II regions, further supporting the view that little mixing of CNO-processed material occurred in the preplanetary envelope of NGC 2392 and the other two planetaries. The low C abundance calculated for NGC 2392 may be an artifact of the use of too high a T_e for the calculation of the C^{++} abundance (see the discussion above), since it is lower than any other object listed and lower than all field planetaries studied by Aller and Czyzak (1983) and than in nearly all the field planetaries tabulated by Pottasch (1984). For reasons discussed above, however, I believe that the weight of the evidence supports the method used to calculate this abundance. The O, Ne, Ar, and S abundances in NGC 1535, NGC 2392, and NGC 6826 are also a bit low, suggesting that NGC 2392, like NGC 1535, NGC 3242, NGC 6826 and NGC 7662, may have formed out of material that was slightly more metal-poor than did the other objects listed in the table.

V. CONCLUSIONS

In summary, NGC 2392 is another planetary nebula for which total abundances can apparently be accurately determined from optical measurements alone. The agreement between the optical and UV abundances of O, N, and Ne is particularly striking; this is especially reassuring for N, where as little as 4% of the N is in the optically observable form of N^+ . As for the other nebulae observed in this series, the UV and optical measurements of the C^{++} abundance do not agree; the fact that this discrepancy is related to ionization state rather than on distance from the central star suggests that the $\lambda 4267$ C II line might be blended with a line of an unknown high-excitation ion. The total abundances in NGC 2392 suggest that it is a planetary nebula that formed initially in a somewhat metal-poor region and has undergone little or no enhancement of its original abundances by mixing with nuclear-processed material.

I am grateful to the *IUE* and Kitt Peak staffs for their assistance in obtaining the observations, to Bruce Balick for several useful discussions and for providing the contour maps of NGC 2392, and to an anonymous referee for several valuable suggestions. The use of the Regional Data Analysis Facility at Goddard is also gratefully acknowledged.

TABLE 1
PARAMETERS OF OBSERVED POSITIONS

PARAMETER	POSITION					
	1	2	3	4	5	6
Offset (arcsec)	4N	7N	10S	11N	3W,17S	13W,17N
c (adopted $c=0.13\pm0.04$)	0.28	0.10	0.12	0.05	0.20	0.02
SWP number	27776	27773	27775	27772	27771	2771
Exposure (min)	75	83	150	120	120	120
LWP number	7708	7713	7712	7707	7706	7706
Exposure (min)	40	120	150	120	120	120
$F(\text{Hg})^a$, 3"4 ent.	3.7 ± 0.4	6.0 ± 0.1	2.0 ± 0.3	2.9 ± 0.2	2.7 ± 0.1	6.3 ± 0.6^b
$F(\lambda 1640)^a$, predicted	4.8 ± 0.7	7.5 ± 0.8	3.7 ± 0.6	4.1 ± 0.7	2.4 ± 0.3	16.:
$F(\lambda 1640)^a$, observed	5.4	7.4	5.6	4.5	3.0	13.4

^aUnits: 10^{-13} ergs cm^{-2} s^{-1} , uncorrected for interstellar extinction.

^bPosition 6 was observed with a larger aperture; see text.

TABLE 2
LINE INTENSITIES

I (λ)

λ (\AA)	ID	f (λ)	Pos.1	Pos.2	Pos.3	Pos.4	Pos.5	Pos.6
1403,1409	O IV]	1.31
1487	N IV]	1.23	78.	29.	67.	42.:
1548,1550	C IV	1.18	54.:	64.	146.	94.	...	99.
1640	He II	1.14	248.	240.	359.	279.	175.	365.
1661,1666	O III]	1.13	59.	75.	70.	79.	25.	82.
1747	N III]	1.12	65.	74.	90.	45.	41.	66.
1906,1909	C III]	1.23	175.	74.	258.	180.	109.	212.
2326,2328	C II]	1.35
2422,2424	[Ne IV]	1.12	105.	57.	94.	86.:	30.	...
3133	O III	0.45	165.	37.:	19.	...	27.	...
3426	[Ne V],0 III	0.38	5.5	5.7	7.5	8.3	2.0	4.3
3444	O III	0.37	6.3	6.4	6.3	6.5	3.3	5.3
3727	[O II]	0.29	120. ^a	90.9 ^a	68.2 ^a	131. ^a	172. ^a	90.9 ^a
3798	H 10	0.27	4.7	5.9	5.6	6.1	5.4	5.7
3835	H 9	0.26	6.1	6.7	7.0	8.1	6.9	7.2
3869	[Ne III]	0.25	96.2	106.	154.	129.	91.4	154.

TABLE 2 cont.

4069-4076	(blend)	0.21	4.1	3.2	2.8	4.9	3.7	2.6
4102	H δ	0.20	24.6	27.4	26.4	28.9	25.2	28.6
4267	C II	0.17	0.37	0.12	1.2:	0.18	0.74	<0.1
4340	H γ	0.15	45.9	48.5	48.5	52.4	45.7	53.2
4363	[O III]	0.15	20.5	23.0	38.1	29.4	15.8	33.4
4471	He I	0.11	3.1	3.2	2.4	3.2	3.4	2.5
4686	He II	0.05	36.0	34.8	52.0	40.5	25.3	52.9
4711	[Ar IV], He I	0.04	2.5	3.2	2.4	4.9	2.1	4.8
4714-26	[Ne IV]	0.04	0.36	0.32	0.75	0.19	0.58:	0.40
4740	[Ar IV]	0.03	1.6	2.1	4.1	2.9	1.4	3.4
4861	H β	0.00	100.	100.	100.	100.	100.	100.
4959	[O III]	-0.03	379.	412.	563.	454.	329.	536.
5007	[O III]	-0.04	1157.	1245.	1716.	1386.	1018.	1604.
5200	[N I]	-0.08	1.2	...	2.8	...
5518	[Cl III]	-0.15	...	0.67	0.72	0.84	0.65	...
5538	[Cl III]	-0.15	...	0.67	0.72	0.67	0.51	...
5755	[N II]	-0.20	2.11	1.21	0.74	1.91	2.36	1.66
5876	He I	-0.22	9.3	8.3	6.0	7.2	10.3	6.7
6300	[O I]	-0.29	1.1	8.7	1.9
6312	[S III]	-0.29	3.7	3.5	4.1	3.7	1.33	4.3
6563	H α	-0.33	313.	286.	295.	295.	307.	261.
6583	[N II]	-0.34	122.	70.1	45.1	91.1	173.	61.3

TABLE 2 continued

6678	He I	-0.35	3.2	2.6	2.2	2.2	3.1	1.2
6717	[S II]	-0.36	8.60	5.01	4.76	6.37	22.3	6.97
6731	[S II]	-0.36	13.2	7.42	5.12	9.41	23.9	7.35
7005	[Ar V]	-0.39
7065	He I	-0.40	3.3	2.7	2.4	2.2	3.2	1.5
7135	[Ar III]	-0.41	13.9	13.4	15.9	13.1	12.5	16.6

^aCorrected for blending; see text.

TABLE 3
ELECTRON TEMPERATURES AND DENSITIES

QUANTITY	ION	RATIO	POSITION					
			1	2	3	4	5	6
N_e (cm^{-3})	S^+	I(6731)/I(6717)	3000	2600	2800	2800	1000	900
N_e (cm^{-3})	Cl^{++}	I(5538)/I(5518)	...	2600	2600	800	800	...
T_e (K)	N^+	I(6583)/I(5755)	10000	10000	9800	10900	9300	12700
T_e (K)	O^{++}	I(5007)/I(4363)	14000	14300	15400	15100	13400	15000
T_e (K)	Ne^{3+}	I(2422)/I(4720)	9300	11000	12600	8200
T_e (K)	H^+	I(Bac)/I(H_β)	...	17000	20800	14500	16300	11400
N_e (adopted)			3000±1000	2600±1000	2800±1000	2800±1000	1000±300	900±300
T_e (X^+ ions)			10000±500	10000±500	9800±500	10900±500	9300±500	12700±600
T_e (X^{++} and higher ions)			14000±600	14300±600	15400±600	15100±600	13400±600	15000±600

TABLE 4
IONIC AND TOTAL ABUNDANCES

λ (Å)	ABUNDANCE	POSITION					
		1	2	3	4	5	6
4471	He ⁺ /H ⁺	0.063	0.065	0.049	0.066	0.069	0.053
5876	He ⁺ /H ⁺	0.069	0.062	0.044	0.054	0.075	0.053
6678	He ⁺ /H ⁺	0.084	0.068	0.057	0.059	0.080	0.033
Average	He ⁺ /H ⁺	0.072	0.065	0.050	0.060	0.075	0.046
4686	He ⁺⁺ /H ⁺	0.030	0.031	0.047	0.036	0.022	0.047
	He/H	0.102±0.008	0.096±0.004	0.097±0.006	0.096±0.007	0.097±0.004	0.093±0.007
3726,3729	10 ⁴ XO ⁺ /H ⁺	0.69	0.50	0.42	0.51	1.03	0.15
5007	10 ⁴ XO ⁺⁺ /H ⁺	1.46	1.49	1.73	1.46	1.44	1.72
1661,1666	10 ⁴ XO ⁺⁺ /H ⁺	2.00	2.21	1.30	1.66	1.13	1.79
	i _{cf}	1.42	1.48	1.94	1.60	1.29	2.02
Optical	10 ⁴ XO/H	3.1±0.4	3.0±0.4	4.2±0.5	3.2±0.4	3.2±0.4	3.8±0.5
6583	10 ⁴ XN ⁺ /H ⁺	0.23	0.13	0.091	0.14	0.39	0.065
1747	10 ⁴ XN ⁺⁺ /H ⁺	0.80	0.80	0.63	0.35	0.67	0.54

TABLE 4 cont.

1487	$10^4 \text{XN}^{3+}/\text{H}^+$	0.98	0.31	0.43	0.31
	i_{cf}	4.42	5.90	9.93	6.18	3.10	25.2
Optical	$10^4 \text{XN}/\text{H}$	1.02 ± 0.2	0.77 ± 0.2	0.90 ± 0.2	0.87 ± 0.2	1.21 ± 0.3	1.64 ± 0.3
UV+Optical	$10^4 \text{XN}/\text{H}$	2.0 ± 0.8	1.2 ± 0.5	1.2 ± 0.5	0.8 ± 0.4	1.1 ± 0.4	0.61 ± 0.3
3869	$10^4 \text{XNe}^{++}/\text{H}^+$	0.31	0.32	0.38	0.33	0.34	0.41
2422	$10^4 \text{XNe}^{3+}/\text{H}^+$	0.40	0.20	0.23	0.23	0.09	...
3426	$10^4 \text{XNe}^{4+}/\text{H}^+$	0.01	0.01	0.01	0.01	0.00	0.01
	i_{cf}	2.09	1.98	2.41	2.16	2.22	2.20
Optical	$10^4 \text{XNe}/\text{H}$	0.65 ± 0.13	0.63 ± 0.13	0.92 ± 0.18	0.71 ± 0.14	0.75 ± 0.15	0.90 ± 0.18
2326,2328	$10^4 \text{XC}^+/\text{H}^+$
1906,1909	$10^4 \text{XC}^{++}/\text{H}^+$	0.44	0.16	0.38	0.30	0.35	0.36
4267	$10^4 \text{XC}^{++}/\text{H}^+$	4.30	1.40	<1.2	2.12	8.50	<1.2
1548,1550	$10^4 \text{XC}^{3+}/\text{H}$	0.09	0.09	0.13	0.09	...	0.10
UV	$10^4 \text{XC}/\text{H}$	0.53 ± 0.20	0.25 ± 0.10	0.51 ± 0.20	0.39 ± 0.16	0.35 ± 0.14	0.46 ± 0.20
7135	$10^6 \text{XAr}^{++}/\text{H}^+$	0.58	0.54	0.56	0.48	0.56	0.61
4740	$10^6 \text{XAr}^{3+}/\text{H}^+$	0.22	0.28	0.45	0.33	0.22	0.41

TABLE 4 cont.

7005	$10^6 \text{XAr}^{4+}/\text{H}^+$
	i_{cf}	1.19	1.12	1.13	1.14	2.01	1.06
Optical	$10^6 \text{XAr}/\text{H}$	0.95 ± 0.15	0.82 ± 0.12	1.58 ± 0.22	1.47 ± 0.20	2.23 ± 0.33	1.47 ± 0.20
6717,6731	$10^6 \text{XS}^+/\text{H}^+$	0.59	0.32	0.33	0.34	1.28	0.18
6312	$10^6 \text{XS}^{++}/\text{H}^+$	3.03	2.69	2.52	2.41	1.27	2.89
	i_{cf}	1.23	1.33	1.54	1.34	1.13	2.06
Optical	$10^6 \text{XS}/\text{H}$	4.5 ± 1.3	4.0 ± 1.2	4.4 ± 1.3	3.7 ± 1.1	2.9 ± 1.0	6.3 ± 2.0

TABLE 5
COMPARISON OF ABUNDANCES

Object	He/H	10^4XO/H	10^4XN/H	10^4XNe/H	10^4XC/H	10^6XAr/H	10^6XS/H	Reference
NGC 2392	0.097±0.001	3.4±0.2	1.1±0.1	0.76±0.05	0.42±0.04	1.4±0.2	4.3±0.5	1
NGC 2392	0.091	3.6	2.1	0.48	2.2	1.3	6.0	2
NGC 1535	0.091	3.7	0.43	0.77	2.7	1.2	...	3
NGC 3242	0.091	4.4	0.91	1.1	2.6	1.4	3.2	4
NGC 6720	0.110	11.2	2.3	1.8	12.	2.4	10.	5
NGC 6826	0.094	4.0	0.51	0.92	3.4	1.3	5.9	6
NGC 6853	0.110	8.4	3.0	2.7	7.6	3.3	5.9	7
NGC 7009	0.117	4.8	1.3	1.5	1.5	2.3	13.	8
NGC 7662	0.094	4.3	1.1	0.9	6.8	1.5	4.2	9
H II regions	0.117	4.0	0.4	1.3	18.	10
Sun	0.100	7.4	0.9	1.1	4.5	3.7	17.	11,12

REFERENCES: (1) This paper. (2) Aller and Keyes (1981). (3) Paper IX. (4) Paper V. (5) Paper VII. (6) Paper VIII. (7) Paper IV. (8) Paper III. (9) Paper VI. (10) Hawley 1978. (11) Ross and Aller 1976. (12) Aller and Czyzak 1983.

REFERENCES

- Aller, L. H., and Czyzak, S. J. 1983, *Ap. J. Suppl.*, **51**, 211.
- Aller, L. H., and Keyes, C. D. 1981, in *The Universe at Ultraviolet Wavelengths* (NASA Conference Publication 2171), 649 (AK).
- _____ . 1980, *Proc. Natl. Acad. Sci. USA*, **77**, No. 3, 1231.
- Balick, B. 1987, *A. J.*, **94**, 671.
- _____ . 1990, private communication.
- Balick, B., and Preston, H., and Icke, V. 1987, *A. J.*, **94**, 1641.
- Barker, T. 1980, *Ap. J.*, **240**, 99 (Paper I).
- _____ . 1982, *Ap. J.*, **253**, 167 (Paper II).
- _____ . 1983, *Ap. J.*, **267**, 630 (Paper III).
- _____ . 1984, *Ap. J.*, **284**, 589 (Paper IV).
- _____ . 1985, *Ap. J.*, **294**, 193 (Paper V).
- _____ . 1986, *Ap. J.*, **308**, 314 (Paper VI).
- _____ . 1987, *Ap. J.*, **322**, 922 (Paper VII).
- _____ . 1988, *Ap. J.*, **326**, 164 (Paper VIII).
- _____ . 1989, *Ap. J.*, **340**, 921 (Paper IX).
- Brocklehurst, M. 1971, *M.N.R.A.S.*, **153**, 471.
- Burstein, D., and Heiles, C. 1982, *A.J.*, **87**, 1165.
- Clegg, R. E. S. 1988, in IAU Symposium 131, ed. S. Torres-Peimbert (Dordrecht: Reidel).
- Hawley, S. A. 1978, *Ap. J.*, **244**, 417.

- Harrington, J. P., Seaton, M. J., Adams, S., and Lutz, J. H. 1982, *M.N.R.A.S.*, **199**, 517.
- Kaler, J. B. 1986, *Ap. J.*, **308**, 337.
- Pottasch, S. R. 1984, *Planetary Nebulae*, (Dordrecht: Reidel), 62.
- Ross, J. E., and Aller, L. H. 1976, *Science*, *191*, 1223.
- Seaton, M. J. 1978, *M.N.R.A.S.*, **185**, 5P.
- Torres-Peimbert, S., and Peimbert, M. 1977, *Rev. Mexicana Astr. Ap.*, **2**, 181.
- Zipoy, D. M. 1976, *Ap. J.*, **209**, 108.

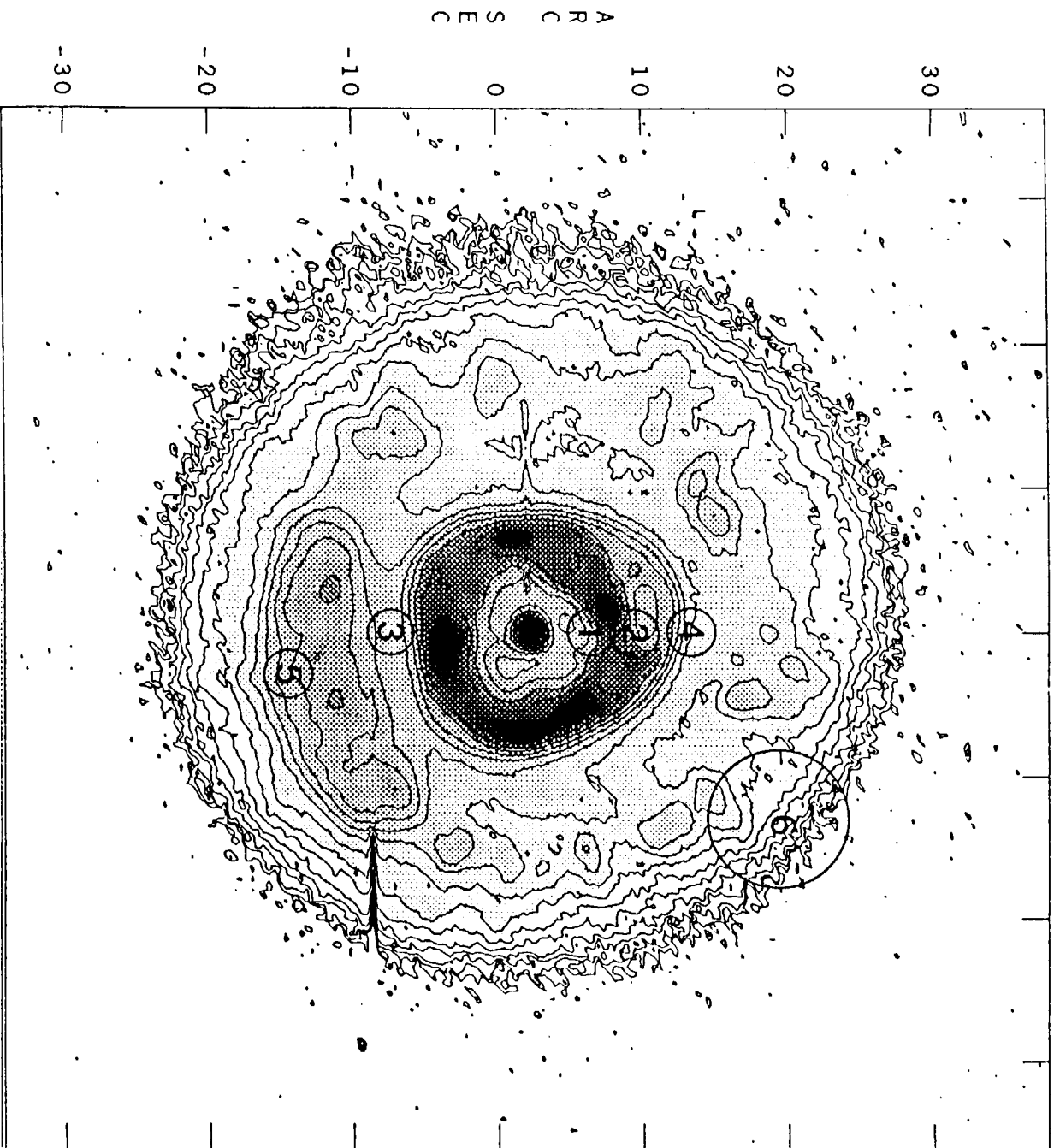
FIG. 1.--An H α contour map of NGC 2392 derived from a 2.1m CCD image as described by Balick (1987). North is up, and east is to the left. The circles indicate the size of the 3."4 diameter entrance aperture used for the optical observations for positions 1-5; a 10."3 diameter aperture was used for position 6. The ultraviolet observations were made in the same positions with apertures of similar sizes; see the text and Table 1 for more details.

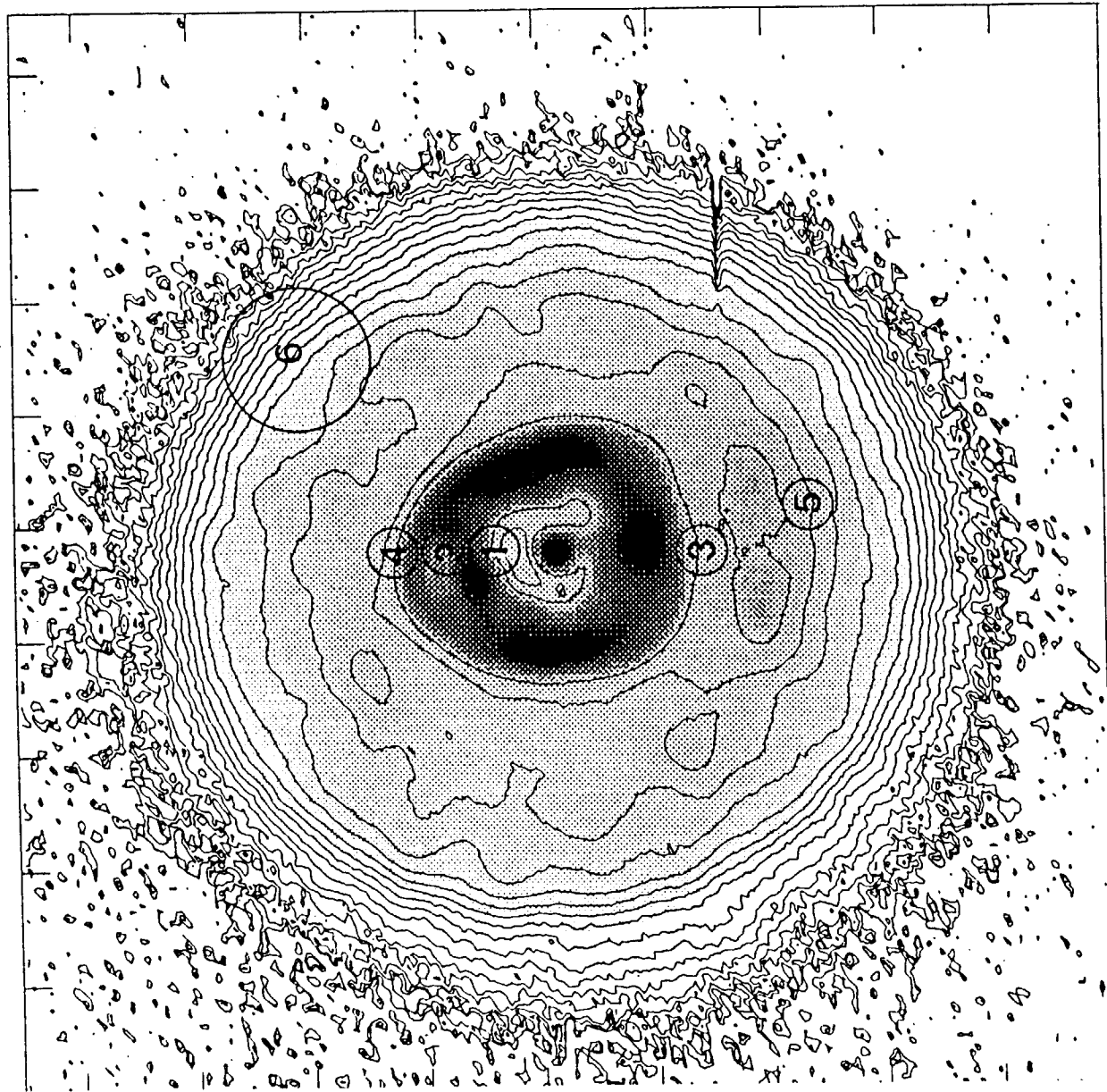
FIG. 2.--Same as Figure 1, but in the light of [O III].

FIG. 3.--Same as Figure 1, but in the light of [N II].

FIG. 4.--Same as Figure 1, but in the light of He II.

TIMOTHY BARKER: Department of Physics and Astronomy,
Wheaton College, Norton, MA 02766





A R C S E C

